Bioresource Technology 200 (2016) 335–341

Contents lists available at ScienceDirect

Bioresource Technology

journal homepage: www.elsevier.com/locate/biortech

A thermogravimetric analysis of the combustion kinetics of karanja (*Pongamia pinnata*) fruit hulls char

Md. Azharul Islam [a,b], M. Auta [a,c], G. Kabir [a], B.H. Hameed [a,*]

[a] School of Chemical Engineering, Engineering Campus, Universiti Sains Malaysia, 14300 Nibong Tebal, Penang, Malaysia
[b] Forestry and Wood Technology Discipline, Khulna University, Khulna 9208, Bangladesh
[c] Department of Chemical Engineering, Federal University of Technology Minna, Nigeria

HIGHLIGHTS

- TGA thermographs traced the KFH-char combustion behaviours.
- Char weight loss shift to higher temperature zones with increasing heating rates.
- Isoconversional methods authenticated the KFH-char combustion kinetics.
- Reaction order and diffusion models dictated the multi-step char combustion.

ARTICLE INFO

Article history:
Received 26 July 2015
Received in revised form 11 September 2015
Accepted 13 September 2015
Available online 9 October 2015

Keywords:
Combustion
Kinetics
Char
Non-isothermal
Thermogravimetry

ABSTRACT

The combustion characteristics of Karanj fruit hulls char (KFH-char) was investigated with thermogravimetry analysis (TGA). The TGA outlined the char combustion thermographs at a different heating rate and isoconversional methods expressed the combustion kinetics. The Kissinger–Akahira–Sunose (KAS) and Flynn–Wall–Ozawa (FWO) methods authenticated the char average activation energy at 62.13 and 68.53 kJ/mol respectively, enough to derive the char to burnout. However, the Coats–Redfern method verified the char combustion via complex multi-step mechanism; the second stage mechanism has 135 kJ/mol average activation energy. The TGA thermographs and kinetic parameters revealed the adequacy of the KFH-char as fuel substrate than its precursor, Karanj fruit hulls (KFH).

1. Introduction

Biomass residues are often loose and have a high oxygen content that seriously limited their energy density for direct use for energy. Therefore, carbonisation processes are beneficial route that convert biomass residues to the biomass char that is attractive for energy (Zhao et al., 2014; Liu et al., 2010). Thermochemical processes, pyrolysis and hydrothermal carbonisation (HTC) convert the biomass lignin and holocellulose via complex reactions wholly to high energy products than the biomass (Chen et al., 2012). The biomass precursor degrades by pyrolysis via concurrent stages, holocellulose decompose between 200 and 380 °C, and lignin component degraded over wide temperatures (180–600 °C) to char (Slopiecka et al., 2012). Thermal stability and structural complexity characterise lignin wide decomposition temperatures; thus, the lignin decomposition reactions is the rate determining step during biomass pyrolysis (Burhenne et al., 2013). Particularly, biomass and theirs chars energy characteristics are established from the procedures prescribed by the American System of Standard and Measurements (ASTM) standards. Futhermore, sufficient knowledge of the thermal decomposition kinetic of biomass, biomass derived-char and coal provides pivotal information to evaluate the feedstocks energy potential. The information is crucial to the design and control of efficient and sustainable thermochemical process that convert the biomass to energy (Damartzis et al., 2011; Ceylan and Topçu, 2014). Thermogravimetry analysis (TGA) received immense patronage in the understanding of solid fuel substrate degradation to release energy. The TGA trace the thermal degradation patterns of fresh biomass, char and hydrochar under air and inert environment for subsequent kinetic studies (Mothé and De Miranda, 2013; Molintas and Gupta, 2011). The patterns revealed the response of heating rates, the inherent biomass properties and severity that defines the char combustion profiles in

* Corresponding author. Tel.: +60 45996422; fax: +60 45941013.
E-mail address: chbassim@usm.my (B.H. Hameed).

http://dx.doi.org/10.1016/j.biortech.2015.09.057
0960-8524/

the form of thermographs (Toptas et al., 2015). From their studies, Azargohar et al. (2014), Meng et al. (2012) outlined a reliable thermal degradability behaviour and reaction kinetic of biomass by TGA based on nonisothermal heating rates. Additionally, Wang et al. (2014) attested the effects of the dissimilar heating rates (non-isothermal single heat rate, non-isothermal multiple heating rate, and isothermal test) on the combustion of four combustions of coal. The heating rates conspicuously interfere with some key parameters, namely activation energies and burnout temperature. Also, the type of kinetics that control the char weight loss over the char combustion temperature programme has direct link to the heating rates. A typical TGA studies revealed that, the differential weight loss of biomass (microalgae) combustion exhibits three stages of weight loss that include dehydration, devolatilisation and char oxidation stages. The whole combustion weight loss shifted to higher temperature zones with increased heating rates during the nonisothermal TGA (Gai et al., 2015). Previously, Sima-Ella et al. (2005) that studied the effects of the both isothermal and non-isothermal heating rate of the thermogravimetric combustion of char presented similar findings. The char combustion weight loss under the non-isothermal temperature programme shifted to higher temperature zones with increased heating rates. Subsequently, the differential weight loss under temperature programme highlighted noteworthy combustion characteristics (ignition, burnout, and peak temperature) for subbituminous coal and palm trees residues (Idris et al., 2012).

In general, char combustion to burnout proceed in stagewise mass transfer mechanisms; firstly, oxygen diffuse to the active char site by chemisorption. Subsequently, the chemisorbed oxygen reacts with the char reactive components, and diffusion mass transfer expel the gas products across the active sites (Zhou et al., 2013; Wu et al., 2014). The mass transfer phenomena facilitate the combustion reaction that leads to the char weight loss. The reactivity of the char during combustion obviously depends on the oxygen diffusion rate, temperature, particle size, char morphology and so on (De La Puente et al., 2000).

To establish a complete picture of the Karanj fruit hulls (KFH) energy application, previously, Islam et al. (2015a) reported the TGA combustion profiles and kinetics of KFH hydrochar prepared by hydrothermal carbonisation. They estimated the kinetics parameters and established the combustion mechanisms of the hydrochar TGA. The hydrochar combustion reactions kinetics parameters and mechanisms were determined using isoconversional Kissinger–Akahira–Sunose (KAS) and Coats–Redfern (CR) methods. Subsequently, this study distinctively aimed to accomplish the wholesome studies to determine the combustion parameters of KFH-char prepared from the pyrolysis of KFH. At heating rates 5, 10, and 20 °C/min, the adequacy of the KFH-char for energy are analysed from solid state kinetic models: isoconversional Flynn–Wall–Ozawa (FWO), KAS and CR methods.

2. Methods

2.1. Materials

The ripen Karanja fruits collected locally, and then using a wooden hammer the seeds and the hull were manually separated. The seed free Karanja fruit hulls (KFH) were washed properly to eliminate dirt. Afterwards, KFH samples were air dried for three days and subsequently dried at 103 ± 2 °C to a constant weight in an oven. The dried KFH-Raw samples were then crushed and sieved to 200–500 μm particle size. The dried crushed KFH materials were carbonised in a vertical tubular stainless steel furnace under purified nitrogen (99.995%) with a flow rate of 150 cm^3/min. The furnace was ramped (10 °C/min) to a constant temperature of 600 °C that was maintained for 1 h. The char product was cooled to room temperature and washed with distilled water several times. Next, the synthesised char named karanja fruit hulls char (KFH-char) dried in an oven at 103 ± 2 °C were stored for subsequent use.

2.2. Methods

The Perkin Elmer TGA 7 was used to determine the moisture content, ash content volatile matter and fixed carbon according to the ASTM (American Society for Testing and Materials) prescribed guidelines. In every case, 5 mg of the sample was used, and the nitrogen flow rate was 20 mL/min; whereas heating rate was retained at 20 °C/min. Perkin Elmer 2400 Series II performed elemental analysis on the KFH-char; it then displayed the tentative elemental compositions of the char.

The combustion process of KFH-char sample was investigated by Perkin Elmer TGA 7. For this, exact amount (5 mg) of KFH-char sample was kept in platinum crucible and heated from 30 to 900 °C in presence of air with three heating rates (5 °C/min, 10 °C/min, and 20 °C/min). The air flow rate was maintained at 20 mL/min. All the experiments were carried out twice to ensure reproducibility.

2.3. Background of kinetic modeling

Kinetic equation for the thermal decomposition reactions of solid state matter is expressed base on rate of conversion as follows:

$$\frac{d\alpha}{dT} = k(T)f(\alpha) \tag{1}$$

where, α is the degree of conversion during thermal decomposition, $d\alpha/dt$ stands for the rate of conversion, t is time, T is the absolute temperature, $k(T)$ is temperature dependent rate constant, and $f(\alpha)$ is the function of reaction mechanism. Then, α can be expressed as Eq. (2).

$$\alpha = \frac{m_o - m_t}{m_o - m_f} \tag{2}$$

where, m_o is the initial mass of the sample, m_f is the final mass of the sample at the end of the reaction, and m_t is the mass of the sample at any time t.

According to Arrhenius law $k(T)$ is the reaction rate constant that may be express as:

$$k(T) = A\exp\left(\frac{-E_a}{RT}\right) \tag{3}$$

where, E_a (J/mol) is the activation energy of the reaction, A is the pre-exponential or frequency factor, R (J/mol k) is the universal gas constant, and T is the absolute temperature.

Eqs. (1) and (3) can be combined to give:

$$\frac{d\alpha}{dT} = A\ \exp\left(\frac{-E_a}{RT}\right)f(\alpha) \tag{4}$$

If the temperature increases with the constant heating rate β (K/s), then $\beta = \frac{dT}{dt} = \frac{dT}{d\alpha} \times \frac{d\alpha}{dt}$ can be introduced to transform Eq. (4) as follows:

$$\frac{d\alpha}{dT} = \frac{A}{\beta}\exp\left(\frac{-E_a}{RT}\right)f(\alpha) \tag{5}$$

The integration function of Eq. (5) is expressed as Eq. (6). Therefore, the Eq. (6) is the fundamental equation that preambled the determination of non-isothermal solid state thermal degradation kinetic methods to determine the kinetic mechanisms parameters.

$$\int_0^\alpha \frac{d\alpha}{f(\alpha)} = g(\alpha) = \frac{A}{\beta}\int_{T_o}^{T} exp^{-\left(\frac{E}{RT}\right)}dT \tag{6}$$

And T is defined as:

$$T = T_o + \beta t \tag{7}$$

where, $g(\alpha)$ is the integral function of conversion and T_o (K) is the initial temperature of the experiment.

Mu et al. (2015) used the isoconversional methods, Kissenger–Akahira–Sunose (KAS) and Flynn–Wall–Ozawa (FWO) to determine the kinetic mechanisms and parameters for solid substrates thermal degradation. Furthermore, Damartzis et al. (2011) used the Coats and Redfern (CR) methods to express the type of reaction mechanisms that tailored the thermal degradation of cardoon. The KAS, FWO and CR methods are often referred as the model-free isoconversional methods. In isoconversional methods, the degree of conversion (α) for a reaction is assumed to be constant such that the rate of reaction depends absolutely on the reaction temperature (T). The methods also does not require any previous knowledge on the mechanism of reaction for degradation of biomass (White et al., 2011). In this study, the methods can be used to determine the thermal degradation kinetic parameters, activation energy (E_a) and pre-exponential factor (A) without prior knowledge of the KFH-char combustion mechanisms. The choice of the methods is based on their reliability in determining the solid state thermal degradation complex mechanisms and kinetic parameters (White et al., 2011; Vyazovkin et al., 2011).

2.4. Kissenger–Akahira–Sunose (KAS) method

The KAS method (Kissinger, 1957; Akahira and Sunose, 1971) expressed as follows:

$$ln\left(\frac{\beta}{T^2}\right) = ln\left(\frac{AE_a}{Rg(\alpha)}\right) - \frac{E_a}{RT} \tag{8}$$

where, the plot of $ln\left(\frac{\beta}{T^2}\right)$ versus $1/T$ gave a straight line from which the slope was used to determine the activation energy E_a.

2.5. Flynn–Wall–Ozawa (FWO) method

The FWO isoconversional method (Ozawa, 1965; Flynn and Wall, 1966) was derived from Doyle's approximation (Doyle, 1961) with Eq. (6), the reaction rate in logarithmic form is expressed as:

$$ln\,\beta = ln\left(\frac{AE_a}{Rg(\alpha)}\right) - 5.331 - 1.052\left(\frac{E_a}{RT}\right) \tag{9}$$

where, the slope of plot $\ln(\beta)$ against $1/T$ at different heating rates can be used to determine the value of apparent activation energy E_a at a constant value of α.

2.6. Coats–Redfern (CR) method

Coats and Redfern (1964) presented model-free method based on isoconversional basis appropriate to describe the thermal decomposition mechanisms for mass loss that is used as an integral kinetic method to describe the reaction process during pyrolysis. The Coats–Redfern method can therefore be used to calculate activation energy, pre-exponential factor, and apparent reaction order. The method is based on Eq. (6) given that $2RT/E_a \to 0$, and then the expression of the Eq. (6) in logarithmic way gives:

$$ln\left(\frac{g(\alpha)}{T^2}\right) = ln\left(\frac{AR}{\beta E}\right) - \frac{E_a}{RT} \tag{10}$$

where, a plot of $ln\left(\frac{g(\alpha)}{T^2}\right)$ against $\frac{1}{T}$ gives a straight line with the pre-exponential factor A deducted from the intercept, and the slope gives the activation energy E_a. The theoretical explanations for the three kinetic mechanisms used to calculate the values of $g(\alpha)$ are presented in Section 3.4. High regression coefficient (R^2) values from the plot informed the adequacy of the mechanisms to the complex kinetics route for the suitable thermal degradation of the solid matter.

3. Results and discussion

3.1. Characteristics of Karanj Fruit hulls char (KFH-char)

The biomass-char physiognomies largely depend on the biomass precursor and nature of the thermochemical process. Of recent, Islam et al. (2015b) hydrothermally carbonised Karanj Fruit hulls (KFH) to hydrochar, named KFH-HTC. In this study, the same KFH substrate experienced arrays of degradation mechanisms under pyrolysis at 600 °C and yielded the KFH-chars. The main chemical constituents of the KFH are ultimately converted to residual bio-oil and syngas, and the net char. The Chars from the pyrolysis and hydrothermal carbonisation have dissimilar compositions and energy densities. Table 1 presented the ultimate and proximate analysis of the KFH-char and KFH precursor. Decarboxylation and dehydration mechanisms deoxygenated the KFH precursor to the KFH-char with vividly lesser oxygen content, and the char heating value exceeded that of the virgin KFH. The higher energy quality of the KFH-char inferred to its high carbon content of 92.22 wt% and lower oxygen (4.13 wt%) content than that of KFH. The surge in carbon and decrease in oxygen improve fuel potential of biomass, the low oxygen and high carbon content yields high energy density of fuel substrates (Kim et al., 2014). The volatile compounds in the KFH-char have 84.17 wt%. The amount compares well with that of lignite coal (Idris et al., 2012); but, higher than that of the virgin KFH and HTC-KFH. The volatile content influences the char ignition temperature during heating application (Toptas et al., 2015). Biomass derived char can have low ignition temperature for its low volatile contents compared to the HTC-KFH with higher volatile content. During thermogravimetric degradation under air, the HTC-KFH can ignite earlier and burn faster to burnout than the KFH-char. On using the same quantity of the two chars for the heating applications, the KFH-char can have longer residence time than the hydrochar. Afterwards, the ultimate analysis revealed a lower sulphur content in the KFH-char (0.08 wt%) than the virgin KFH (0.36 wt%) and KFH-HTC. The notable corrosion effect and the toxic substance emission to the environment are unlikely during the burning of the char for energy (Hu et al., 2015). The char hydrogen/carbon ratio (0.039) less than that of the hydrochar signifies dissimilar CO_2 emission from the gases per unit energy produced. Relatively, coal hydrogen/carbon ratio (0.084) (Idris et al., 2010) showed a wider margin of a difference than with the hydrochar following the char having the highest carbon content.

3.2. Thermogravimetric analysis of karanja fruit hulls char (KFH-char)

Non-isothermal TGA presented valuable thermographs that interpret the combustion behaviour to evaluated biomass and biomass-derived char for energy (Ounas et al., 2011). Thermographs offered to elucidate the complexities in the thermal degradation of the fuel substrates and their precursors. Consequently, the combustion kinetic are deduced from the information offered by the thermographs for use in the design and control of combustion furnaces for heating applications (Zhou et al., 2013).

Figs. 1 and 2 are the KFH-char TGA thermographs that revealed the change in weight loss and extent of conversion patterns with increasing temperature. The graphs showed the vivid influences of heating rates on the oxidation of the char via combustion; the

Table 1
Characteristics of KFH-char.

Sample	Elemental analysis (wt%)					Proximate analysis (wt%)				Reference
	Carbon	Hydrogen	Nitrogen	Oxygen*	Sulphur	Moisture	Volatile matter	Fixed carbon	Ash	
KFH	45.10	6.13	–	48.41	0.36	3.71	84.17	6.33	5.79	(Islam et al., 2015b)
KFH-char	92.22	3.57	–	4.13	0.08	4.033	13.984	72.985	8.988	This study

* By difference.

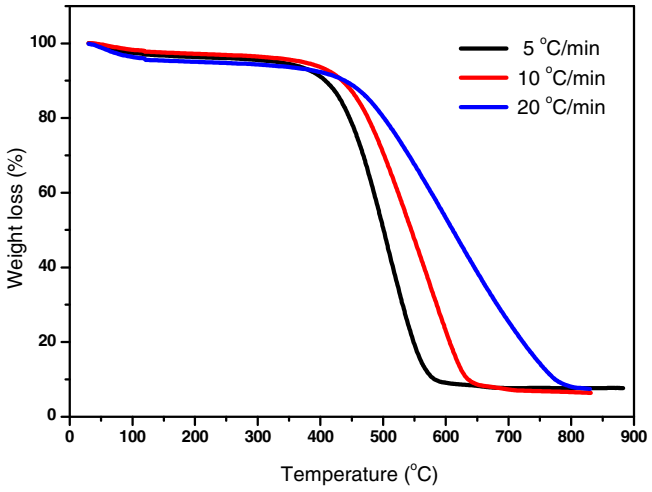

Fig. 1. Effect of heating rates on weight loss KFH-char under air.

heating rates favoured the concurrent chemical reaction mechanisms for the rapid char oxidation. The heat permeates and volatilises the char against the impending heat transfer restrictions that can limit the char oxidation mechanisms. The oxidation reactions perpetuate the life cycle of the char that hinged on the char burnout conditions at a distinct heating rate. Often depending on the heating rates, the burnouts of the chars are attained sooner at a lower temperature or in the later at a higher temperature. The char characteristics coupled with TGA residence time and severity exhibited to affect the char lifecycle. Correspondingly, the literature (Idris et al., 2012) that examined the TGA of biomass and lignite coal, and their blends highlighted similar behaviour as the burnout is attained.

Fig. 3 is the resultant of Fig. 1, it presents the derivative weight loss curves for the KFH-char oxidation at three distinct heating rates during the TGA. The thermographs established two different regions of the char volatilisation. The curves characterised the char combustion via their burnout temperatures and peak temperatures at least and maximum rate devolatilisation respectively. Subsequently, Table 2 displayed the temperature intervals for the distinct combustion regions and weight losses at the corresponding heating rates deduced from Fig. 3. The first stage at 30–400 °C favoured to oxidise the volatile matters against the small mass and heat transfer restrictions. The volatile matters are oxidised based on the chemical reaction that passively led the slight weight loss in the char at the respective heating rates. The corresponding weight losses during the passive combustion stage shown in Table 2, limited from 6.31 to 8.795 wt% for the heating rates of 5–20 °C/min. However, the second stage that signified the char combustion zone are narrowed in specific temperature intervals (as in Table 3) at the respective heating rate. The second stage is the most active that constituted wholesome speedy devolatilisation of the carbon-rich KFH-char to burnout. The heating rate of 5, 10 and 20 °C/min stimulate the char to volatilised to a corresponding weight loss of 82.0, 82.6 and 84.3 wt%. Furthermore, the KFH-chars reactivity is credited to their intrinsic compositions dominated by carbon in considerable excess than the volatiles matters accrued during preparation and handling. The char oxidation region persisted over broad temperature for the heating rates of the TGA studies (see Fig. 3 and Table 3). The stage also facilitates the release of sufficient energy from the char combustion up to its entire burnout.

Relatively, the KFH-HTC hydrochar oxidation thermographs exhibited three stages (Islam et al., 2015a) contrary to the two stages exhibited by KFH-char. The hydrochar distinct components, cellulose and lignin, are simultaneously volatilised to char in the second stage, and the char decomposed in the third stage to burnout. On the contrary, the KFH-char combustion follows the consecutive devolatilisation of the instilled high carbon content

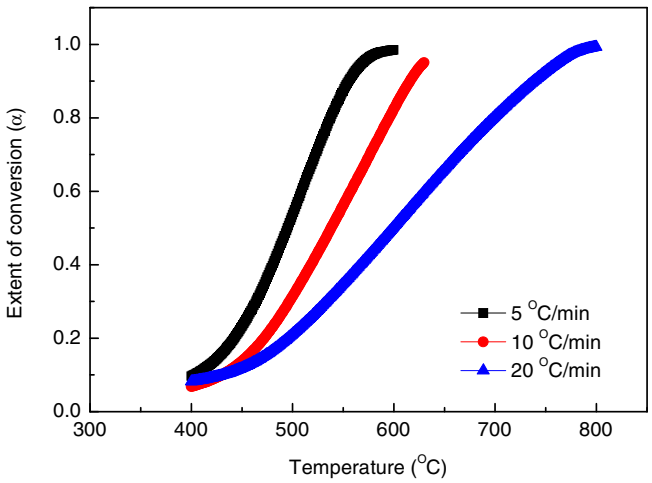

Fig. 2. Temperature versus α of all samples at different heating rates.

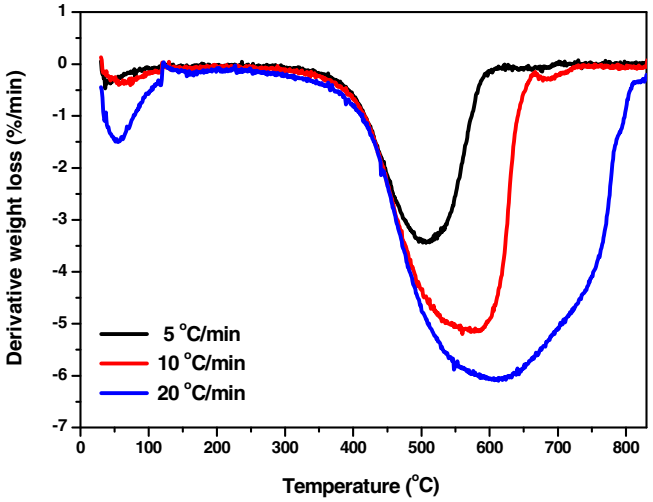

Fig. 3. Effect of heating rates on derivative weight loss of KFH-char under air.

Table 2
Temperature intervals for different regions.

Heating rate (°C/min)	Temperature intervals (°C)		Weight loss of samples, % by weight	
	First region	Second region	First region	Second region
5	30–400	400–600	8.795	82.001
10	30–400	400–630	6.31	82.555
20	30–400	400–800	7.658	84.271

and volatile matters within the char morphology by pyrolysis in the second and first stage respectively.

3.3. Effect of heating rate on the peak and burnout temperature

The effects of heating rates on fuel substrate combustion peak and burnout temperatures are inherent knowledge for the design of efficient combustion furnace. The combustion thermographs of derivative weight loss pointed out the maximum rate of weight loss at corresponding peak temperature. As the heating persist, the fuel residue volatilised further from the peak temperature to burnout at temperature synonymous to stagnant weight loss.

Fig. 3 showed the KFH-char thermographs of derivative weight loss at corresponding heating rates; Table 3 presented the effect of heating rate on the KFH-char combustion peak and burnout temperatures. The lowest and highest temperature on the KFH-char thermographs disclosed the burnout temperatures to be 600 and 800 °C at 5 and 20 °C/min heating rate respectively. Also, the curves showed that the upsurge in the heating rate from 5 to 20 °C/min did not favour the rise in combustion activities of the KFH-char. As it is preferable, the chars burn at a lower heating rate (5 °C/min). At a higher heating rate, heat transfer across the char particles is effective, but limited by the impending heat transfer resistances. However, at a lower heating rate, the residence time was adequate for heat to permeate steadily into the KFH-char particles amidst the limiting resistance layer. These observations are in agreement with what were in the literature (Idris et al., 2010). The corresponding temperatures at the maximum rate of weight loss were 507, 569 and 613 °C for 5, 10 and 20 °C/min heating rate respectively from the derivative weight loss curves in Fig. 3.

The fact that the char witnessed two stages of combustion, the results of the first and second stage weight loss of the KFH-char combustion in Table 3 are compatible as in Fig. 3. The dual stages of the char's derivative weight loss at the respective characteristic temperatures ranges and peaks revealed the complexity nature of the KFH-char combustion. In stage two, the broad peaks signified the high activity that rapidly oxidised the char via increased ability to overwhelm the mass transfer resistance layer. The phenomena explain the dominance of the chemical reaction that controlled the char volatilisation that accelerates the release of heat energy. Therefore, the stagewise degradation activities of the char particles are coherent with the literature (Wu et al., 2014). Oxygen permeates the KFH-char diffusion layer overcome the mass transfer resistance to volatilise the char, in contrast to that under pyrolysis that need only heat permeability to degrade the char. The oxygen disperses in and outside the char particles to aids the maximum char rate of weight loss at the peak temperature. Away from the peak combustion rate at 507–613 °C the mass transfer resistance continuously build-up, and seriously limit the penetration of the oxygen to promote the burning. Subsequently, at the burnout, the diffusion layer becomes stringent to the oxygen permeability; finally stagnated weight loss to signify the end of the char lifecycle. Also, on approaching burnout the char particles noticed inconsistent heat distribution that led to prolong heating with a rise in heating rates. The phenomena observed are coherent with a report in the literature (Hu et al., 2015).

Table 3
Peak temperature and burn out temperature (°C).

Heating rate (°C/min)	Peak temperature (°C) Second region	Burn out temperature (°C)
5	507	600
10	569	630
20	613	800

Furthermore, the start to the end of the weight loss during the KFH-char TGA signifies the life cycle or burnout time for the char during combustion. The KFH-char burnout temperature is higher compared to those of KFH raw and KFH-HTC biomass; also, connoted longer residence time (Idris et al., 2012). The attribute led to the slow reaction between KFH-char, and the air enhance the dilution nitrogen gas and argon of the air constituents (Molintas and Gupta, 2011). Table 3 showed the increasing burnout temperature from 600 to 800 °C for the increasing heating rate of 5–20 °C/min, respectively. In particular, the highest burnout temperature was 800 °C for 20 °C/min heating rate, 630 °C and 600 °C for 10 °C/min and 5 °C/min heating rate respectively.

Relatively, the KFH-HTC combustion proceeded to burnout in the characteristic pattern as exhibited by the KFH-char. Also, (Wu et al., 2014) confirmed similar observations on the burnout temperature increases with a rise in heating rates for the oxidation of biomass by TGA process. The scenario can persist as volatility temperature of the part near the char surface before the particle core is attained. Consequently, the KFH-char particle experience uneven distribution of heat at the higher heating rate.

3.4. Kinetic study

The KFH-char combustion kinetic evaluated from the isoconversional methods is now presented. The methods resolve the consternation of getting a large variance (errors) in the kinetic parameters of similar biomass species against other models (White et al., 2011). The systematic error that emanate while estimating the activation energy and pre-exponential constant are restricted with isoconversional kinetic methods, Flynn–Wall–Ozawa (FWO), Kis singer–Akahira–Sunose (KAS) and Coats–Redfern (CR). Fig. 4 presented the plots of the FWO and KAS methods at various degrees of conversion. The kinetic parameters, apparent activation energies and pre-exponential constants in Table 4 are from the slopes and intercepts of the plots.

The KFH-char activation energy values from the isoconversional KAS and FWO methods are 62.13 and 72.41 kJ/mol, respectively. Drying of the Karanja fruit hulls before conversion to char, and thermal combustion of the resultant char enhanced ample decomposition of its volatile component thereby facilitating the spontaneous rate of reaction. The dissimilar apparent activation energy 36–106 kJ/mol and 49–112 kJ/mol from the KAS and FWO methods, respectively hinged on the complex multi-step KFH-char combustion mechanisms. Consequently, the methods certainly clarify the dependence of the entire char TGA decomposition on the activation energies. The increase in the degree of conversion was accompanied by a decrease in the energy of activation as it is evident in Table 4. The extent of char conversion increased from 0.1 to 0.8 with a corresponding reduction in activation energy of resolved by KAS and FWO methods, respectively. The coherence or reliability of the kinetic parameters from the KAS and FWO methods are apparent from the high correlation coefficients (0.9582 to 0.9999). The good fitted linear plots of conversion ratios shown in Fig. 4 showed the adequacy of the kinetic parameters from the char combustion by TGA. A similar observa-

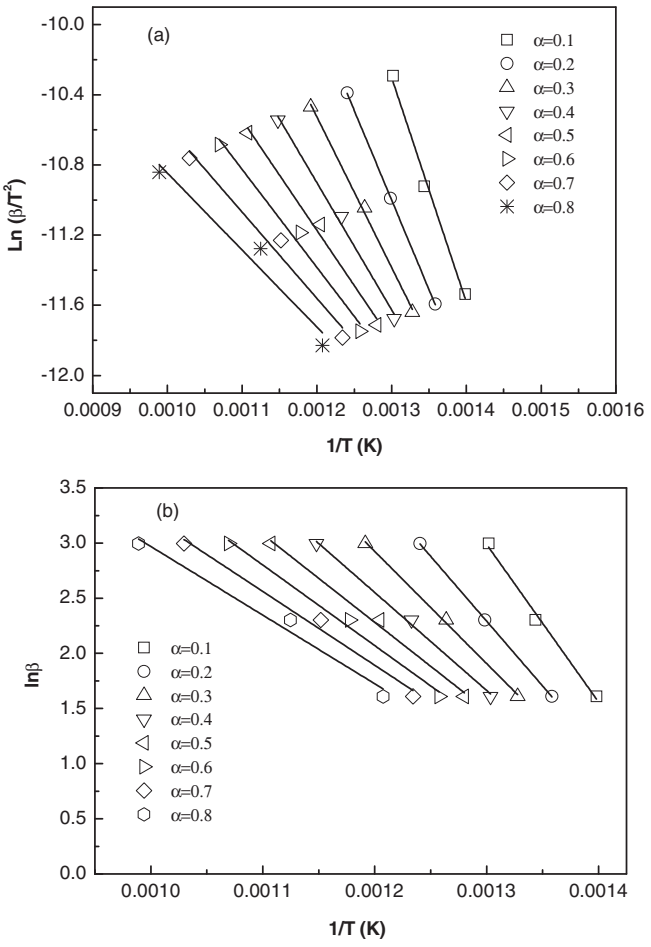

Fig. 4. Isoconversional plots at various conversion degrees (α) for KFH-char by (a) KAS and (b) FWO methods.

tion was made with the kinetic study of poplar wood pyrolysis (Slopiecka et al., 2012).

At the inception of the nonisothermal TGA process, it is intrinsic that the low temperature of the KFH-char combustion leads low fractional conversion. The trend observed follows from the inadequate kinetic control mechanism to drive the decomposition faster. However, at high temperature, the lower activation energy hasten the progress of the char decomposition towards the peak temperatures of Fig. 3. The rapid increase in the char combustion is favoured by the transit from mass diffusion to adequate kinetic control mechanism towards the char burnout. The consequence is contrary at the char burnout temperatures; where there is sufficient build-up of the mass diffusion mechanism over the kinetic control mechanism that restricted the rapid char degradation. The scenario of stagnant decomposition of the char manifested, and the weight loss remain constant as at the end of the second stage of the char thermogravimetric combustion. The resultant ash in the vicinity of the char particles can be inert to the burning, but can constitute resistance to both mass and heat transfers across the char particles. On the contrary during pyrolysis, the char decomposition can be catalysed by the ash (Wang et al., 2014).

Table 5 presents the apparent activation energies of KFH-char combustion obtained by Coats–Redfern method (CR). The energies are critical in the control of the progress of the non-isothermal thermogravimetric combustion of the KFH-char. During the second stage char degradation, the CR third-order kinetic (F_3) has the largest values of activation energy (135.83 kJ/mol) than the first (F_1) and second order (F_2) kinetics, 70.50 and 99.70 kJ/mol, respectively. The F_1 kinetic is the dominant mechanism of the reaction model kinetics during the char combustion; contrary to the F_3 with the highest activation energy. Furthermore, activation energies from the diffusion kinetics models D_1–D_4 can also assert significant influence on the char degradation under air. The D_3 kinetic with the least activation energy prevailed in influencing the char combustion than the D_1, D_2 and D_4 kinetics. The reliability of the activation energies values from the different kinetic based on their

Table 4
Activation energy (E) and pre-exponential factors (A) by Kissinger–Akahira–Sunose (KAS) and Flynn–Wall–Ozawa (FWO) method.

Conversion (α)	Kissinger–Akahira–Sunose			Flynn–Wall–Ozawa		
	E_{KAS}, (kJ/mol)	R^2	A (min^{-1})	E_{FWO}, (kJ/mol)	R^2	A (min^{-1})
0.1	106	0.9933	5.91E+05	112.927	0.9944	2.85E+06
0.2	85	0.9999	1.65E+04	92.877	0.9999	1.31E+05
0.3	71	0.9979	1.87E+03	80.406	0.9987	2.17E+04
0.4	60	0.9953	3.30E+02	70.208	0.9972	5.52E+03
0.5	52	0.9906	1.03E+02	63.021	0.9947	2.33E+03
0.6	46	0.9856	4.71E+01	57.755	0.9925	1.39E+03
0.7	41	0.9746	2.51E+01	52.876	0.9876	9.72E+02
0.8	36	0.9582	1.94E+01	49.174	0.9809	9.65E+02

Table 5
Theoretical expressions of $g(\alpha)$ (White et al., 2011) and kinetics parameters obtained by Coats–Redfern (CR) method.

Mechanism (White et al., 2011)	$g(\alpha)$	2nd zone		
		E (kJ/mol)	A (min^{-1})	R^2
Reaction order models				
First-order (F1)	$-\ln(1-\alpha)$	70.489	8.91E+01	0.9954
Second-order (F2)	$(1-\alpha)-1-1$	99.718	1.73E+04	0.9554
Third-order (F3)	$[(1-\alpha)-2-1]/2$	135.834	1.01E+07	0.9016
Diffusion models				
One way transport (D1)	α^2	112.263	2.00E+04	0.9876
Two way transport (D2)	$[(1-\alpha)\ln(1-\alpha)]+\alpha$	123.695	7.79E+04	0.9947
Three way transport Jander (D3)	$[1-(1-\alpha)^{1/3}]^2$	55.707	3.83E+00	0.9937
Ginstling–Brounshtein (D4)	$1-(2\alpha/3)-(1-\alpha)^{2/3}$	128.459	4.04E+04	0.9967

correlation values connotes the char combustion following complex multi-step kinetic to burnout.

Comparatively, KFH-HTC hydrochar (Islam et al., 2015a) burns under air via complex multiple-steps kinetic mechanisms in a similar manner as the KFH-char. However, dissimilar activation energies from the same models favour their combustion. Wang et al. (2011) reported the thermal decomposition of blended coal; they asserted that the multi-step mechanisms encouraged the coal thermal decomposition. Similar, assertion was made by Idris et al. (2012) for the burning of coal dotted with biomass during the TGA. Also, the authors (Gil et al., 2010) stressed their conclusion for the burning of the various substrates and their precursors on the reliability of the CR isoconversional method.

4. Conclusion

Characterisations and thermogravimetry analysis under air defined the energy potential of the KFH-char from the KFH pyrolysis. The char have enhanced fuel quality due to its higher carbon (92.20%) and lower sulphur (0.08%) than KFH. The KFH-char combustion kinetics reveals dissimilar activation energy, 106–36 kJ/mol and 112–49 kJ/mol from KAS and FWO methods respectively. The degree of char conversion increase with increasing temperature; since the activation energies diminish to encourage the rapid char degradation. The reaction order and diffusion models of the CR method disclosed the firm dependence of the char combustion on a complex multi-step mechanism.

Acknowledgements

The authors acknowledge the research grants provided by the Universiti Sains Malaysia, under Research University (RU) grant (Project No: 1001/PJKIMIA/814227) that resulted in this article.

References

Akahira, T., Sunose, T., 1971. Joint convention of four electrical institutes. Sci. Technol. 16, 22–31.
Azargohar, R. et al., 2014. Effects of temperature on the physicochemical characteristics of fast pyrolysis bio-chars derived from Canadian waste biomass. Fuel 125, 90–100.
Burhenne, L. et al., 2013. The effect of the biomass components lignin, cellulose and hemicellulose on TGA and fixed bed pyrolysis. J. Anal. Appl. Pyrolysis 101, 177–184.
Ceylan, S., Topçu, Y., 2014. Pyrolysis kinetics of hazelnut husk using thermogravimetric analysis. Bioresour. Technol. 156, 182–188.
Chen, C., Ma, X., He, Y., 2012. Co-pyrolysis characteristics of microalgae Chlorella vulgaris and coal through TGA. Bioresour. Technol. 117, 264–273.
Coats, A.W., Redfern, J.P., 1964. Kinetic parameters from thermogravimetric data. Nature 201 (4914), 68–69.
Damartzis, T. et al., 2011. Thermal degradation studies and kinetic modeling of cardoon (Cynara cardunculus) pyrolysis using thermogravimetric analysis (TGA). Bioresour. Technol. 102 (10), 6230–6238.
De La Puente, G., Fuente, E., Pis, J.J., 2000. Reactivity of pyrolysis chars related to precursor coal chemistry. J. Anal. Appl. Pyrolysis 53 (1), 81–93.
Doyle, C.D., 1961. Kinetic analysis of thermogravimetric data. J. Appl. Polym. Sci. 5, 285–292.
Flynn, J.H., Wall, L.A., 1966. A quick, direct method for the determination of activation energy from thermogravimetric data. Polym. Lett. 4, 323–328.
Gai, C. et al., 2015. Combustion behavior and kinetics of low-lipid microalgae via thermogravimetric analysis. Bioresour. Technol. 181, 148–154.
Gil, M.V. et al., 2010. Thermal behaviour and kinetics of coal/biomass blends during co-combustion. Bioresour. Technol. 101 (14), 5601–5608.
Hu, M. et al., 2015. Thermogravimetric study on pyrolysis kinetics of Chlorella pyrenoidosa and bloom-forming cyanobacteria. Bioresour. Technol. 177, 41–50.
Idris, S.S. et al., 2010. Investigation on thermochemical behaviour of low rank Malaysian coal, oil palm biomass and their blends during pyrolysis via thermogravimetric analysis (TGA). Bioresour. Technol. 101 (12), 4584–4592.
Idris, S.S., Rahman, N.A., Ismail, K., 2012. Combustion characteristics of Malaysian oil palm biomass, sub-bituminous coal and their respective blends via thermogravimetric analysis (TGA). Bioresour. Technol. 123, 581–591.
Islam, M.A., Kabir, G., Asif, M., Hameed, B.H., 2015a. Combustion kinetics of hydrochar produced from hydrothermal carbonisation of Karanj (*Pongamia pinnata*) fruit hulls via thermogravimetric analysis. Bioresour. Technol. 194, 14–20.
Islam, M.A., Asif, M., Hameed, B.H., 2015b. Pyrolysis kinetics of raw and hydrothermally carbonized Karanj (*Pongamia pinnata*) fruit hulls via thermogravimetric analysis. Bioresour. Technol. 179C, 227–233.
Kim, S.S., Shenoy, A., Agblevor, F.A., 2014. Thermogravimetric and kinetic study of Pinyon pine in the various gases. Bioresour. Technol. 156, 297–302.
Kissinger, H.E., 1957. Reaction kinetics in differential thermal analysis. Anal. Chem. 29, 1702–1706.
Liu, Z., Zhang, F.S., Wu, J., 2010. Characterization and application of chars produced from pinewood pyrolysis and hydrothermal treatment. Fuel 89 (2), 510–514.
Meng, X. et al., 2012. Combustion study of partially gasified willow and DDGS chars using TG analysis and COMSOL modeling. Biomass Bioenergy 39, 356–369.
Molintas, H., Gupta, A.K., 2011. Kinetic study for the reduction of residual char particles using oxygen and air. Appl. Energy 88 (1), 306–315.
Mothé, C.G., De Miranda, I.C., 2013. Study of kinetic parameters of thermal decomposition of bagasse and sugarcane straw using Friedman and Ozawa–Flynn–Wall isoconversional methods. J. Therm. Anal. Calorim. 113 (2), 497–505.
Mu, L. et al., 2015. Pyrolysis behaviors and kinetics of refining and chemicals wastewater, lignite and their blends through TGA. Bioresour. Technol. 180, 22–31.
Ounas, A. et al., 2011. Pyrolysis of olive residue and sugar cane bagasse: non-isothermal thermogravimetric kinetic analysis. Bioresour. Technol. 102 (24), 11234–11238.
Ozawa, T., 1965. A new method of analyzing thermogravimetric data. Bull. Chem. Soc. Jpn. 38, 1881–1886.
Sima-Ella, E., Yuan, G., Mays, T., 2005. A simple kinetic analysis to determine the intrinsic reactivity of coal chars. Fuel 84 (14–15), 1920–1925.
Slopiecka, K., Bartocci, P., Fantozzi, F., 2012. Thermogravimetric analysis and kinetic study of poplar wood pyrolysis. Appl. Energy 97, 491–497.
Toptas, A. et al., 2015. Combustion behavior of different kinds of torrefied biomass and their blends with lignite. Bioresour. Technol. 177, 328–336.
Vyazovkin, S. et al., 2011. ICTAC Kinetics Committee recommendations for performing kinetic computations on thermal analysis data. Thermochim. Acta 520, 1–19.
Wang, C.A. et al., 2011. A study on coal properties and combustion characteristics of blended coals in northwestern China. Energy Fuels 25 (8), 3634–3645.
Wang, G. et al., 2014. Thermogravimetric analysis of coal char combustion kinetics. J. Iron Steel Res. Int. 21, 897–904.
White, J.E., Catallo, W.J., Legendre, B.L., 2011. Biomass pyrolysis kinetics: a comparative critical review with relevant agricultural residue case studies. J. Anal. Appl. Pyrolysis 91 (1), 1–33.
Wu, K. et al., 2014. Pyrolysis characteristics and kinetics of aquatic biomass using thermogravimetric analyzer. Bioresour. Technol. 163, 18–25.
Zhao, P. et al., 2014. Clean solid biofuel production from high moisture content waste biomass employing hydrothermal treatment. Appl. Energy 131, 345–367.
Zhou, Z. et al., 2013. Oxy-fuel combustion characteristics and kinetic parameters of lignite coal from thermo-gravimetric data. Thermochim. Acta 553, 54–59.